Supporting Information

Staudigel et al. 10.1073/pnas.1421052112

Abiotic and Biotic Glass Alteration

Microcorrosion textures in volcanic glass are interpreted as biogenic partly because of their uniquely biological shapes (1) but also because they are very different from well-understood abiotic glass alteration textures (see ref. 2 for a review). Hence it is important to understand abiotic glass alteration textures as well as textures that are interpreted as biogenic. Abiotic glass alteration involves the formation of hydration rinds on the surfaces of basaltic glass where anhydrous and noncrystalline glass transforms into palagonite. In thin sections, palagonite appears as a very distinct deep yellow birefringent material that is easily distinguished from the isotropic, largely clear, honey-colored glass (Fig. S1). Palagonite alteration fronts typically progress into the glass along smooth surfaces parallel to the exterior surface, where glass has access to circulating water, occasionally rounding off sharp corners inside a glass particle. Overall, this process is understood as a hydration and chemical exchange reaction with no or negligible congruent (wholesale) dissolution. Biotic alteration, however, invariably involves congruent dissolution of cavities with no or minimal hydration and incongruent dissolution (Figs. S2 and S3).

In Fig. S2 we show a series of scanning electron microphotographs of cracks with granular alteration pitting, using different magnifications (Fig. S2 *A* and *B*) and displaying a range of developmental stages of granular textures, from individual near-spherical micrometer-sized corrosion pits (Fig. S2*B*) to clusters of such pits (Fig. S2*C*) and tens of microns of thick accumulation of such pits along a crack surface (Fig. S2*D*). Edges of such spherical pits along the crack surfaces are commonly sharp, and their interiors are filled with smectite. Tubular textures typically extend at relatively steep angles from exterior or crack surfaces into the glass, typically 1-μm-thick and many tens of micrometers to 150-μm-long (Fig. S3). Tubes may be scarce and relatively short during initial stages of tubular alteration (Fig. S3*A*), forming an increasingly dense network with increasingly longer tubes (Fig. S3 *B* and *C*). They may also merge with and interact with varioles (Fig. S3 *C* and *D*). Tubular textures may emerge from a layer of granular alteration that may itself emerge from a palagonite rind on the fracture surface (Fig. S4).

Sharp edges of granular alteration pits and tunnels and the well-constrained diameters of tubular textures and the lack of palagonite along the surfaces suggest a targeted dissolution process rather than diffusive glass hydration. Such targeted dissolution is feasible either by preferred dissolution along preexisting weakness in the glass or a specific alteration process that is capable of targeting and directing local dissolution of glass at rates faster than the formation of hydration rinds. Preexisting weaknesses are an unlikely explanation because corrosion damage never mirrors across adjacent sides of cracks and because it is hard to imagine a primary weakness in shapes of a spiral or an annulated tube. However, targeted dissolution of rocks by colonizing microbes is a well-established process for soil feldspars (3) or in the dissolution of rock surfaces from lichens, including rock drilling by fungi and by bacteria (4). Hence, biogenicity appears as the most likely interpretation of these textures.

Bioalteration textures may also be preserved as titanite replacements in formerly glassy basaltic rocks from greenstone belts such as in Barberton/South Africa (Fig. S5) or the Pilbara/Australia (Fig. S6). Fig. S5 shows a series of thin-section photographs of biotextures in a glassy pillow margin now replaced by fine-grained chlorite. Overview and detailed images in Fig. S5 show the context of biotextures in relation to a now-healed former crack (Fig. S5 *A*–*C*) and details of segmented and chlorite overgrown tubes. It is important to note that titanite is a common metamorphic mineral that is exclusively associated with not only biotextures but also abiotic features such as varioles (Fig. S5*C*, *Insert*). Biotextures from the Euro Basalt (Pilbara, Australia) (Fig. S6 *A*–*C*) are associated with the exterior surfaces of a (chlorite-replaced) glass shard, expressed here in a paler green chlorite matrix than in the upper and lower portion of the image. Some of the nearly opaque titanite-enriched areas develop distinct tubular textures (Fig. S5 *B* and *C*), whereas others do not. Such a spectrum of titanite textures is best explained by many processes, some of which may or may not have a biological component to them. It is important to recognize that they cannot in their entirety be explained by a simple abiotic or biotic process.

There are many reasons why it is challenging to recognize bioalteration in Archean rocks (i.e., older than 2.5 billion years), and this difficulty also implies that some minimum criteria are considered, without which biogenicity should not be accepted. Key among those is the burden of proof that the observed titanite textures are related to (former) cracks in the glass or the surface of glass shards. Furthermore, only very distinct textural features can be uniquely related to biotic processes such as thin, formerly tubular textures. Biogenicity of purely granular alteration is more difficult to prove. Also it has to be accepted that some titanites replace features that are clearly of abiotic origin, such as the near-spherical varioles.

1. McLoughlin N, Furnes H, Banerjee NR, Muehlenbachs K, Staudigel H (2009) Ichnotaxonomy of microbial trace fossils in volcanic glass. *J Geol Soc London* 166:159–169.
2. Staudigel H, et al. (2008) 3.5 billion years of glass bioalteration: Volcanic rocks as a basis for microbial life? *Earth Sci Rev* 89:156–176.
3. Jongmans AG, van Breemen N, Lundstrom U (1997) Rock-eating fungi. *Nature* 389(6652):682–683.
4. Banciu HL (2013) Diversity of endolithic prokaryotes living in stone monuments. *UBB Biologia, LVIII* 1:99–109.

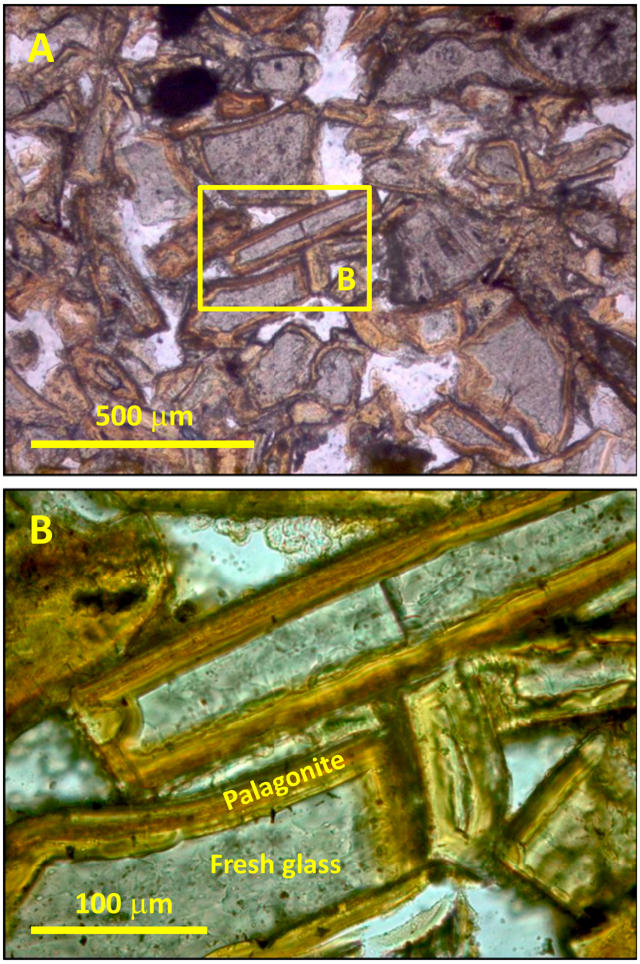

Fig. S1. Photomicrograph of a sample from a Quaternary subglacial hyaloclastite (basaltic glass sand, sample number 73–24-I) from the pillow lava/hyaloclastite mountain Mosfell (located 15 km northeast of Reykjavik, Iceland). Yellowish brown palagonite rinds form an outer layer around the clear glassy cores of glass shards. The white interstitial material is zeolite. The boxed area of *A* is shown as an enlarged image in *B*.

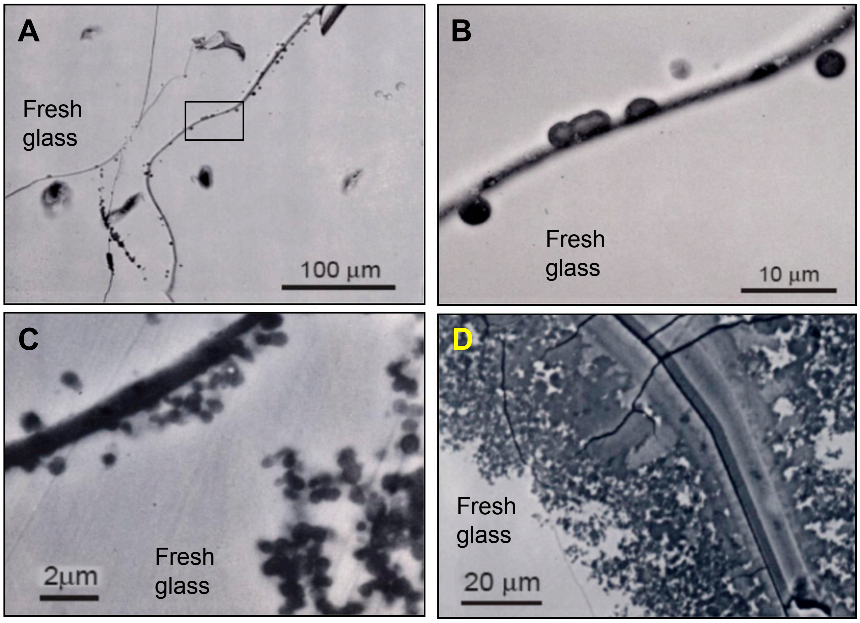

Fig. S2. Scanning electron microscope (SEM) images showing progressive development of granular texture along fractures, from an incipient stage (*A* and *B*) to moderately advanced stage (*C*) and highly advanced stage (*D*). *B* is an enlarged part from *A*. Samples *A* and *B* are from ocean drilling project (ODP) site 648B-1R-1, unit 3, piece 7, 37–40 cm. Sample *C* is from DSDP site 418A-52–5, 75–80 cm, and sample *D* is from DSDP site 417D, 30–6, 20–24 cm.

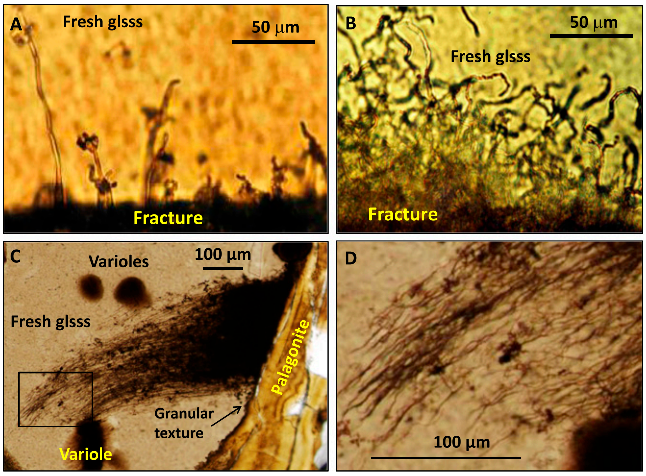

Fig. S3. Thin-section images of tubular structures (all rooted in fractures) in fresh basaltic glass from pillow lava rims from in situ ocean floor. (*A*) Beginning growth stage of tubes, oriented at approximately a right angle to the fracture. Image is from DSDP sample 70–504B, 35–1, piece 274, 106–113. (*B*) Random orientation of tubes. Image is from ODP sample 48.896A, 11R-1, piece 10, 111–113 cm. (*C*) Dense population of tubes. Image is from DSDP sample 418A, 62–4, 64–70 cm. At the root zone of the tubular texture and at the boundary between the fresh glass and palagonite is a relatively thin layer of granular texture. Three varioles, surrounded by fresh glass, are shown. (*D*) Details from *C*.

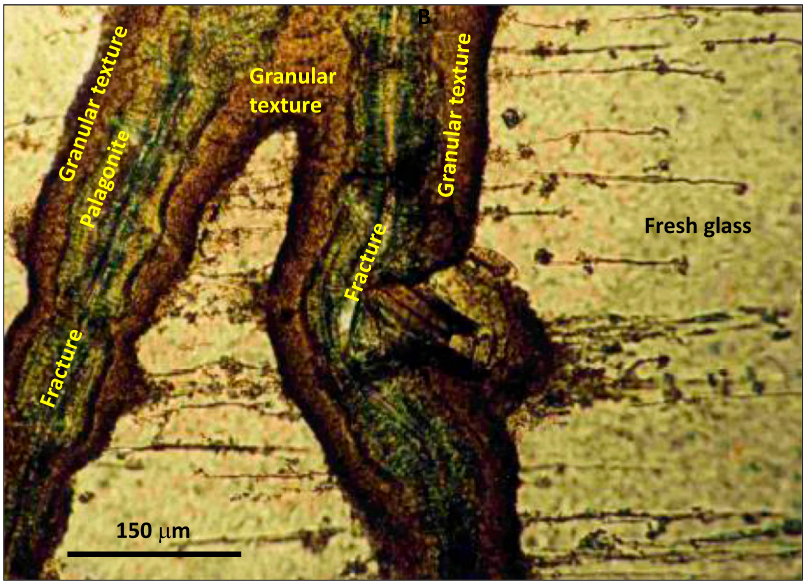

Fig. S4. Thin-section photograph of preferred alignment of thin and long tubes, independent of the orientation of fractures. Image is from DSDP sample 70–504B, 47–2, piece 889, 123–124. Note that adjacent to the fractures is palagonite, formed as the first stage of alteration, likely when the ambient temperature was too high for microbial settlement. Later, when thermal conditions permitted microbial colonization, granular texture developed adjacent to the palagonite rinds. At the latest stage is the growth of the tubular structures.

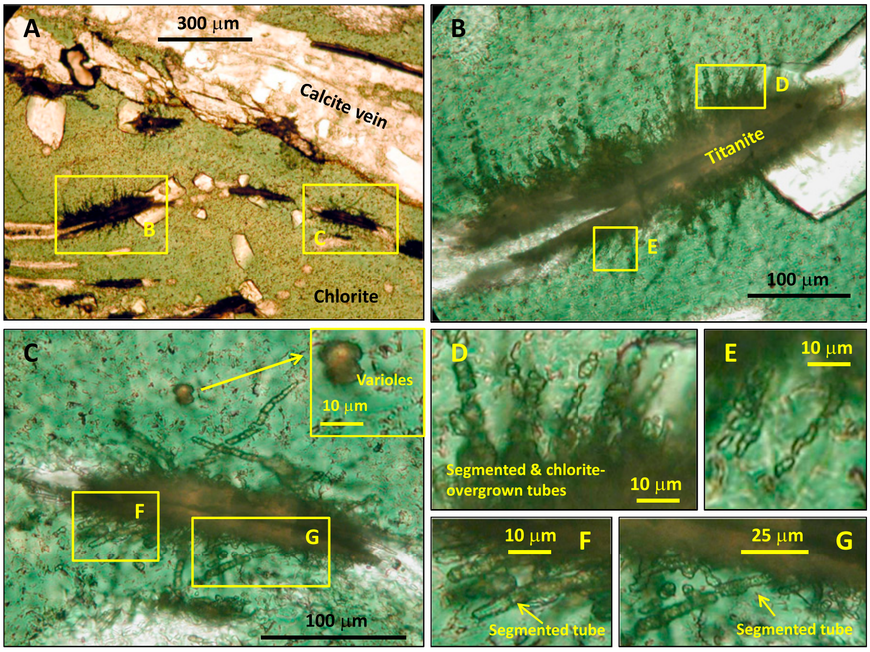

Fig. S5. (*A*) Photomicrograph of pillow rim (from sample 29-BG-03) collected from the uppermost part of the Hooggenoeg Complex. The original glass, replaced by chlorite (yellowish green), exhibits several fractures that have been partly healed by the growth of chlorite. Across the lower middle part of the photomicrograph is a partly healed fracture, along which several dark brown patches of mainly fine-grained titanite are rooted. Projecting out from these titanite patches are numerous micrometer-sized tubular structures. From two of these patches (boxed and labeled *B* and *C*) all of the measurements of the widths of the tubular structures, shown in Fig. 2*B*, have been done. (*B* and *C*) Enlarged photos of the two titanite patches (from *A*) showing the numerous tubular textures projecting into the original glass (now chlorite), predominantly at a right angle to the fracture in which they are rooted and have grown, but some also have oblique angles to the fracture. In the upper right corner of *C* (boxed) is an enlarged picture of two coalesced varioles, around 10 µm in diameter. Note that these bodies are entirely surrounded by chlorite (the original glass). *D*–*G* show details from the tubular structures, demonstrating segmentation and chlorite overgrowth.

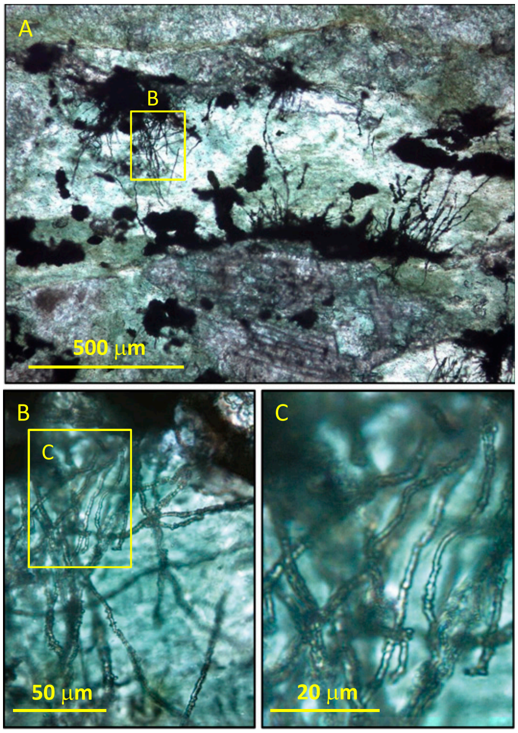

Fig. S6. (*A*) Photomicrograph showing tubular structures in interpillow hyaloclastite (sample 74-PG-04) from the 3.35 Ga Euro Basalt of the PC, Western Australia. The black zones of titanite show the location of healed boundaries between originally glassy fragments, along which the tubular structures are rooted. The fine-grained light green material is chlorite, and the white to light brownish material is calcite. (*B*) Details from *A* that show the complex texture and intertwined character of the tubular structures. Note the octopus-like structures in the central part of the picture. (*C*) Details from *B* that show the segmented nature of the tubular structures.